

Wideband Polarization Conversion Based on Elliptical-Shaped Metasurface for X-Band Applications

Ayktun COSKUN^{1*}, Ahmet TEBER², Mehmet ERTUGRUL³

¹Bayburt University, Vocational School of Technical Sciences, Electronics and Automation Department, Bayburt, Turkey

²Bayburt University, Vocational School of Technical Sciences, Electricity and Energy Department, Bayburt, Turkey

³Ataturk University, Engineering Faculty, Electrical Electronics Department, Erzurum, Turkey

Received:12/12/2022, Revised:23/08/2023, Accepted: 05/10/2023, Published: 31/12/2023

Abstract

Here, a single-layer, ultra-thin, multi-functional and high efficiency meta-surface is presented to perform wideband reflective linear (LP) and circular polarization (CP) transformations. The proposed meta-surface behaves as an excellent cross polarization converter for linear polarized wave over the relative absorption bandwidth (RAB) of 55.2% (7.89–13.91 GHz) with more than 97% efficiency. It successfully converts linearly polarized waves into circularly polarized waves in the 7.2–7.36 GHz frequency range. In addition, its polarization conversion rate (PCR) efficiency characteristics for TE and TM modes are retained across the entire X band, with a wide incidence angle up to 45°. The presented polarization converter has ultra-thin feature with 0.07λ₀ thickness. Due to its compact size, angular stability, high efficiency, simple structure and multi-functionality, this polarization converter is an important candidate for polarization manipulation and communication devices in many applications.

Keywords: Polarization converter, metasurface, cross polarization conversion, PCR, X band

Eliptik Şekilli Metayüzeve Dayalı Geniş Bant Polarizasyon Dönüşümü

Öz

Burada, geniş bant yansıtıcı doğrusal polarizasyon (LP) ve dairesel polarizasyon (CP) dönüşümlerini gerçekleştirmek için tek katmanlı, ultra ince, çok işlevli ve yüksek verimli bir meta-yüze sunulmaktadır. Önerilen meta-yüze, %97'den fazla verimlilikle %55.2'lik (7.89-13.91 GHz) nispi absorpsiyon bant genişliği (RAB) üzerinde doğrusal polarize dalga için mükemmel bir çapraz polarizasyon dönüştürücü görevi görür. Doğrusal polarize dalgaları 7.2–7.36 GHz frekans aralığında başarıyla dairesel polarize dalgalara dönüştürür. Ek olarak, TE ve TM modları için polarizasyon dönüşüm oranı (PCR) verimlilik özellikleri, 45°'ye kadar geniş bir geliş açısı ile tüm X bandında korunur. Sunulan polarizasyon dönüştürücü, 0.07λ₀ kalınlık ile ultra ince bir özelliğe sahiptir. Kompakt boyutu, açısal kararlılığı, yüksek verimliliği, basit yapısı ve çok işlevliliği nedeniyle bu polarizasyon dönüştürücü, birçok uygulamada polarizasyon manipülasyonu ve iletişim cihazları için önemli bir adaydır.

Anahtar Kelimeler: Polarizasyon dönüştürücü, metayüze, çapraz polarizasyon dönüşümü, PCR, X bant

*Corresponding Author: aykut25coskun@gmail.com

Ayktun COSKUN, <https://orcid.org/0000-0002-7240-6865>

Ahmet TEBER, <https://orcid.org/0000-0002-7361-2302>

Mehmet ERTUGRUL, <https://orcid.org/0000-0003-1921-7704>

1. Introduction

Polarization, phase, frequency, and amplitude are the fundamental components of electromagnetic (EM) wave [1-2]. Effective control of the polarization direction is essential for the use of EM waves in microwave, optical and visible regimes. For polarization manipulation and control, polarization converters utilizing crystals' optical activity and the Faraday effect may be used [3]. However, they can exhibit undesirable behaviors such as bulky volume, high sensitivity to incidence angle, and narrow band. Meta-surface-based polarization transducers, which have gained popularity in recent years, attract attention to eliminate such undesirable behaviors [4].

There exist crucial applications of meta-surfaces on the enhancement of antenna radiation [5], reducing radar cross-section [6], real-time holograms [7], flat lensing [8], radio frequency identification (RFID) tags without chips [9], beam splitters [10], plane waves [11], mutual coupling reduction in antenna arrays [12], absorbers [13] and polarization converters [14]. These meta-surfaces make it simple to alter the receiving wave polarization in the reflection or transmission mode. Meta-surfaces based on transmission-mode are generally constructed on a multilayer form. Thus, their production is time-consuming, difficult, and costly. However, meta-surfaces based on reflection mode generally have a single-layer structure.

In recent years, single-layer meta-surfaces based on reflection mode and used as polarization converters have gained great interest and popularity in various fields of study. These fields can be listed as follows: linear polarization (LP) to circular polarization (CP), CP to CP, and LP to LP. They can be constructed in various forms including V-shape [15], W-shape [16], L-shape [17], U-shape [18] and split-ring-resonator shape [19]. However, it is still insufficient to achieve efficiency improvement, bandwidth expansion, functionality expansion and angle insensitivity simultaneously in a facile design so far.

In this study, a meta-surface based on polarization converter is proposed to perform wide-band reflective LP-to-CP transformations in conjunction with X-band. The presented converter both provides effective broadband cross polarization conversion (CPC), and LP-CP. An effective broadband cross-polarization conversion (CPC), and LP-CP conversion are obtained by the presented converter. Besides the surface current distributions of the presented meta-surface are examined.

2. Material and Methods

2.1. Geometrical Configuration

Fig. 1 represents the unit cell of the presented converter. As known, geometric parameters and their configurations must be carefully optimized to obtain reasonable/feasible polarization converter properties so that the incidence power can be attributed to a reflective meta-surface. The bottom portion of the FR-4 substrate is completely coated in copper, while the top surface of the FR-4 is covered with copper as two diagonally symmetric sectors. Copper is used to create an elliptical structure and the ground, whereas the thickness (t) is 0.035 mm, and the conductivity (σ) value is 5.96×10^7 S/m. The other material used in this study is the FR-4 with

a thickness of $0.07\lambda_0$ including the dielectric constant ($\epsilon_r=4.3$) and dissipation factor ($\tan\delta$) value of 0.025. The center of the elliptical structure is positioned in the middle of the top surface of the substrate including the optimum design parameters, which is shown in Table 1. A magnitude and a resonant frequency range can be editable by the geometry, dimension, thickness, and structure properties. With that manner, the optimization process what we have done in this study is carried out obtaining the better absorption by altering the substrate thickness (h) and the parameters ($R_1, R_2, d, P, h,$ and t) of elliptical structures.

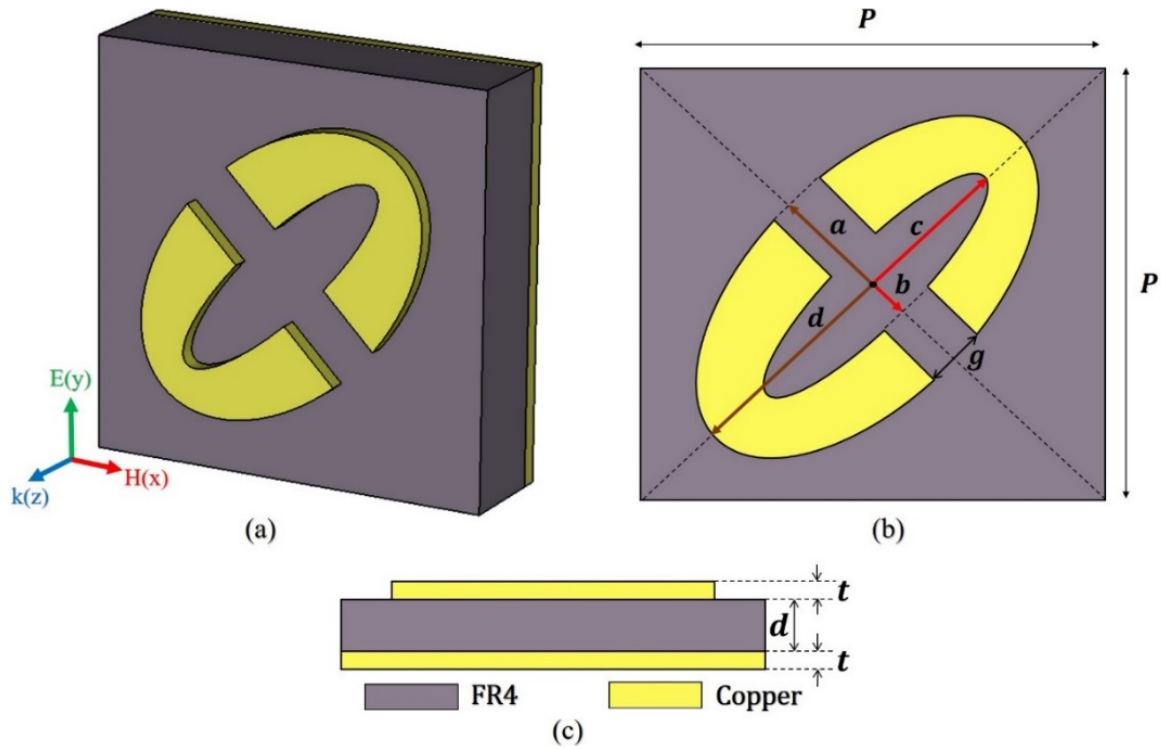


Figure 1. Dimensions of the suggested converter. (a) Top view. (b) Top view including dimension parameters. (c) Side view.

Table 1. Dimensions of the suggested polarization converter (mm).

R_1	R_2	d	P	h	t
0.5	0.9	3.6	12.4	8.4	0.035

2.2. Reflection Coefficients

The electromagnetic wave that is reflected from the converter mostly consists of the co- and cross-polarized reflected fields. Assuming that for the incident field \mathbf{E}_i linearly polarized in the x-axis ($\mathbf{E}_i = \vec{x}E_{ix}$), one can obtain $R_{yx} = |E_{ry}| / |E_{rx}|$ and $R_{xx} = |E_{rx}| / |E_{rx}|$. Similarly, the incident field \mathbf{E}_i linearly polarized in the y-axis ($\mathbf{E}_i = \vec{y}E_{iy}$), the co- and cross-polarized components are demonstrated via $R_{xy} = |E_{rx}| / |E_{ry}|$ and $R_{yy} = |E_{ry}| / |E_{ry}|$, respectively. Here, E_{rx} and E_{ry} are the components of reflected electric field in the x- and y-axes. Therefore,

in mathematical expression, the Jones reflection coefficient matrix [R] for the Cartesian system is showed [4] by:

$$R = \begin{bmatrix} R_{xx} & R_{xy} \\ R_{yx} & R_{yy} \end{bmatrix}$$

An important measure of CPC is the polarization conversion rate (PCR) for the incident y-polarization, defined as [1]:

$$PCR = \frac{|R_{xy}|^2}{|R_{xy}|^2 + |R_{yy}|^2}$$

Stokes equations were used to determine whether the reflected wave was right-hand (RHCP) or left-hand circular polarization (LHCP) [3].

$$e = \frac{2|R_{xy}||R_{yy}|\sin\Delta\Phi_1}{|R_{xy}|^2 + |R_{yy}|^2}$$

The reflected wave is RHCP when the normalized ellipticity is +1 ($R_{xy}=R_{yy}$ and $\Delta\Phi_1=90^\circ + 2k\pi$ (k is integer)). The reflected wave is LHCP when the normalized ellipticity is -1 ($R_{xy}=R_{yy}$ and $\Delta\Phi_1=-90^\circ + 2k\pi$ (k is integer)).

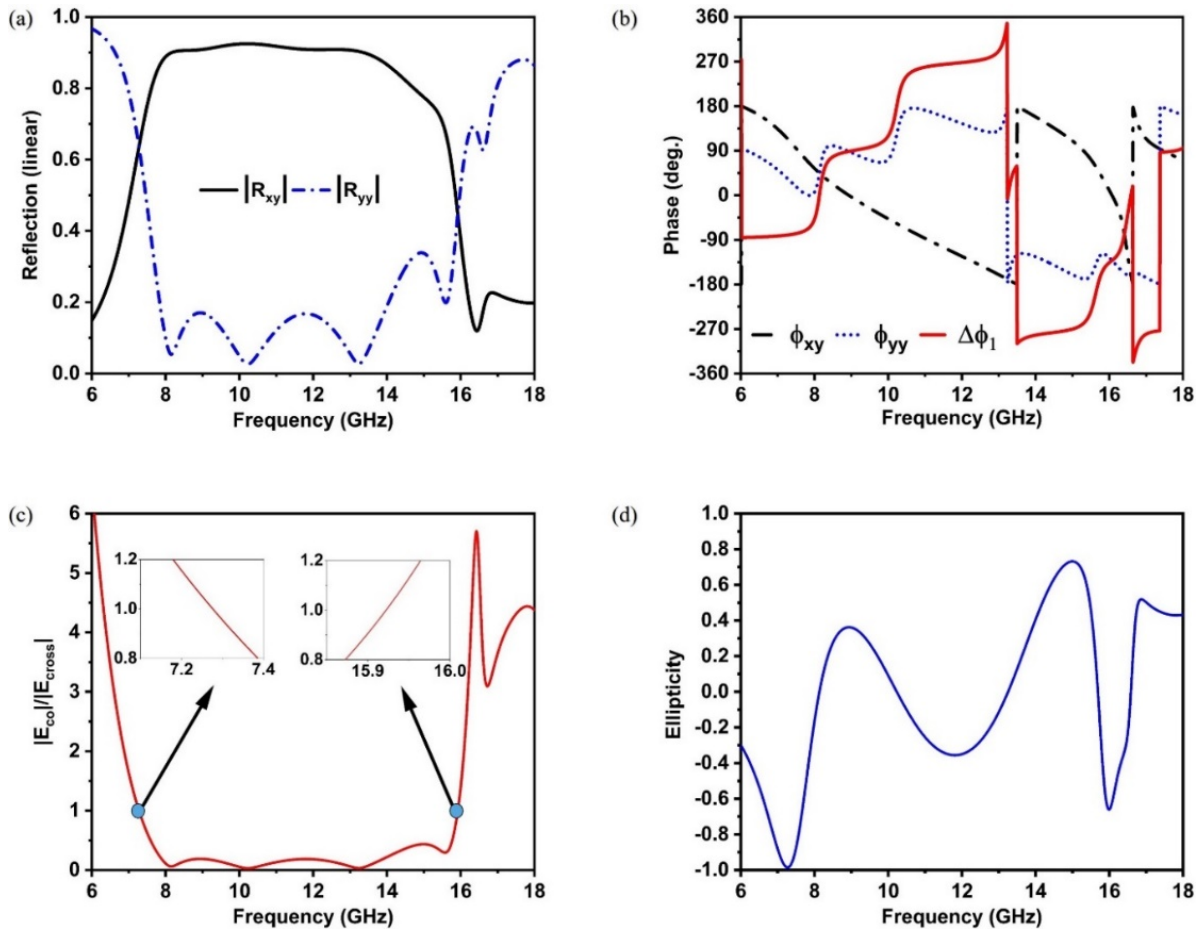


Figure 2. (a) $|R_{xy}|$ and $|R_{yy}|$, (b) ϕ_{xy} , ϕ_{yy} , and $\Delta\phi_1$, (c) $|E_{co}|/|E_{cross}|$, and (d) Ellipticity (e) of the presented metasurface.

2.3. Eigen-polarization and Eigenvalue

Eigenvalues and eigen-polarization of the presented meta-surface are investigated to figure out the cross-polarization conversion. The polarization transform can better be solved by eigen-polarizations and the eigenvalues which can be calculated from [4]:

$$\mathbf{R}\mathbf{X} - m\mathbf{X} = 0$$

where \mathbf{R} is the matrix of reflection coefficient, \mathbf{X} is the eigenvector, and m is the eigenvalue. Here, the assumption was that the cross-polarized reflections are neglected as the ideal case. While the eigenvalues for the \mathbf{R} matrix are $e^{i0} = 1$ and $e^{i\pi} = -1$, the eigenvectors for the \mathbf{R} matrix are $u = [1 \ 1]^T$ and $v = [-1 \ 1]^T$, respectively. Here, the superscript ‘ T ’ denotes the transpose operation on matrices.

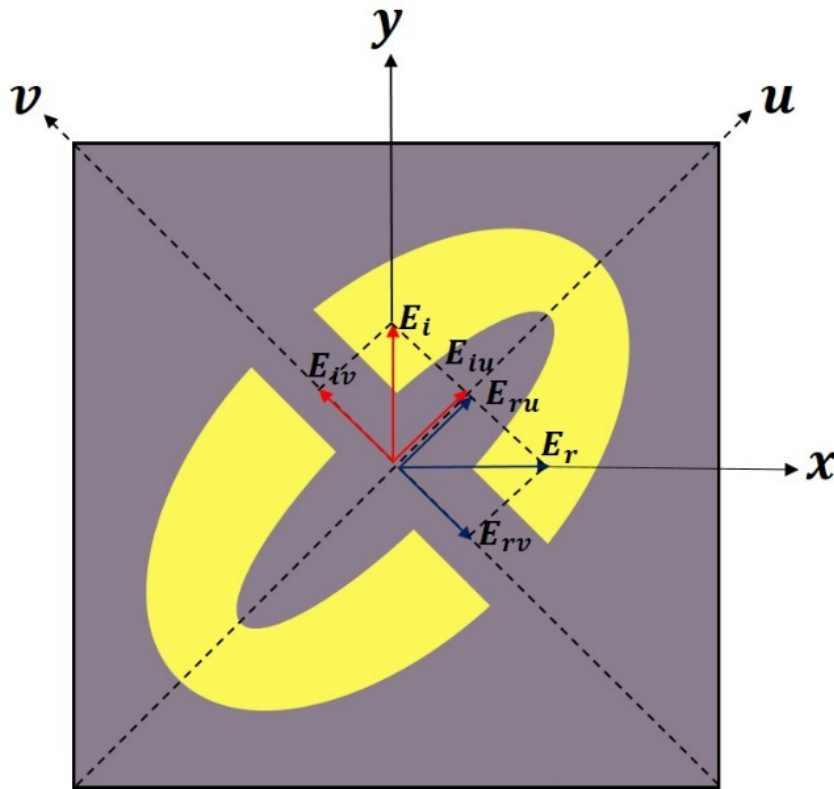


Figure 3. Orthogonal components of the electric field in the u and v directions.

In Fig. 3, it is assumed that the linear polarized field along the u and v axes with an orientation of $\pm 45^\circ$ with regard to the x or y axes is reflected back without any conversion. For the incident field E_i linearly polarized in the y -axis, the reflected field E_r can be written as [1]:

$$E_i = \hat{y}E_i = \hat{u}E_{iu} + \hat{v}E_{iv}$$

$$E_r = \hat{u}E_{ru} + \hat{v}E_{rv} = \hat{u}r_u E_{iu} + \hat{v}r_v E_{iv}$$

Here, the components of the incident electric field (E_{iu} and E_{iv}) are described in the u- and v-axes, respectively while the components of the reflected electric field (E_{ru} and E_{rv}) are identified in the u- and v-axes, respectively. It has been demonstrated in a recent study [4] that it is possible to express: E_r as

$$E_r = \hat{u}(r_{uu}E_{iu}e^{i\phi_{uu}}+r_{uv}E_{iv}e^{i\phi_{uv}}) + \hat{v}((r_{vv}E_{iv}e^{i\phi_{vv}}+r_{vu}E_{iu}e^{i\phi_{vu}})$$

where r_{uu} , r_{vv} , r_{uv} , and r_{vu} denote the components of reflection coefficients in u- and v-axes.

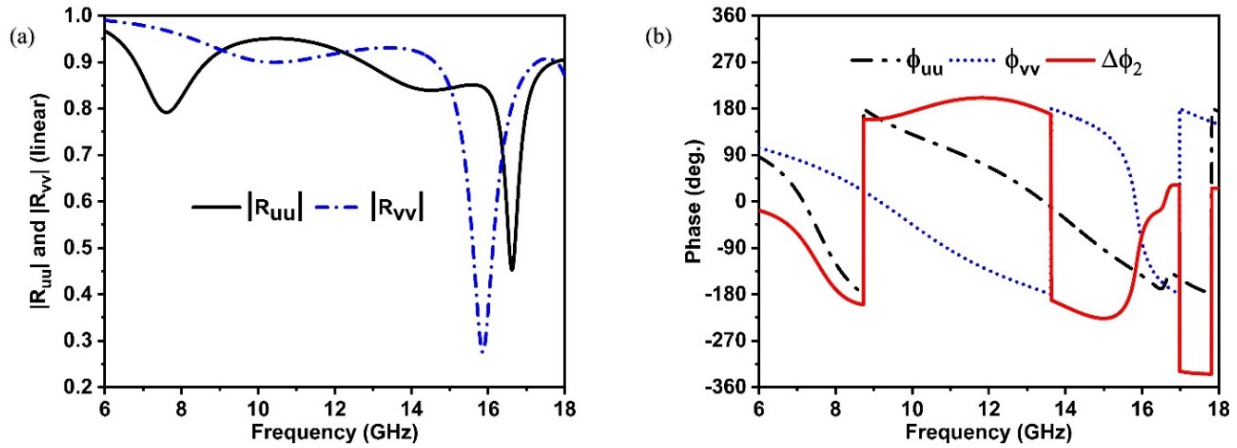


Figure 4. Values of (a) $|R_{uu}|$ and $|R_{vv}|$ and (b) ϕ_{uu} , ϕ_{vv} , and $\Delta\phi_2$ of the suggested metasurface.

3. Results and Discussion

3.1. Geometrical Configuration

Outcomes of the analysis of the efficiency of the presented meta-surface were performed by CST Microwave Studio. It is observed from Fig. 2(a) that $|R_{xy}|$ and $|R_{yy}|$ are, respectively, greater than 0.88 and less than 0.16 for the frequency region between 7.89 and 13.91. It is also noted from the results in Fig. 2(c) that the reflection coefficients of co- and cross-polarization reach equivalent magnitudes at 7.26 GHz and 15.94 GHz. As observed from Figs. 2(b) and 2(d), different frequency dependence of $\Delta\phi_1$ produces different e values over the entire frequency band. It is seen from Fig. 2(d) that the reflected wave has circular polarization property at one discrete frequency at 7.25 GHz with right-handed circular polarizations.

On the other hand, Figs. 4(a) and 4(b) show the magnitude and phase variations of R_{uu} and R_{vv} together with $\Delta\phi_2 = \phi_{uu} - \phi_{vv}$ where ϕ_{uu} and ϕ_{vv} are the phases of R_{uu} and R_{vv} . Firstly, both $|R_{uu}|$ and $|R_{vv}|$ have large values below approximately 15 GHz. While the value of $|R_{uu}|$ is greater than 0.79 up to 16.24 GHz, the value of $|R_{vv}|$ is greater than 0.9 up to 14.76 GHz. Secondly, $\Delta\phi_2 \approx \pm 180^\circ$ all of the X-band, which is considered as a good polarization converter property.

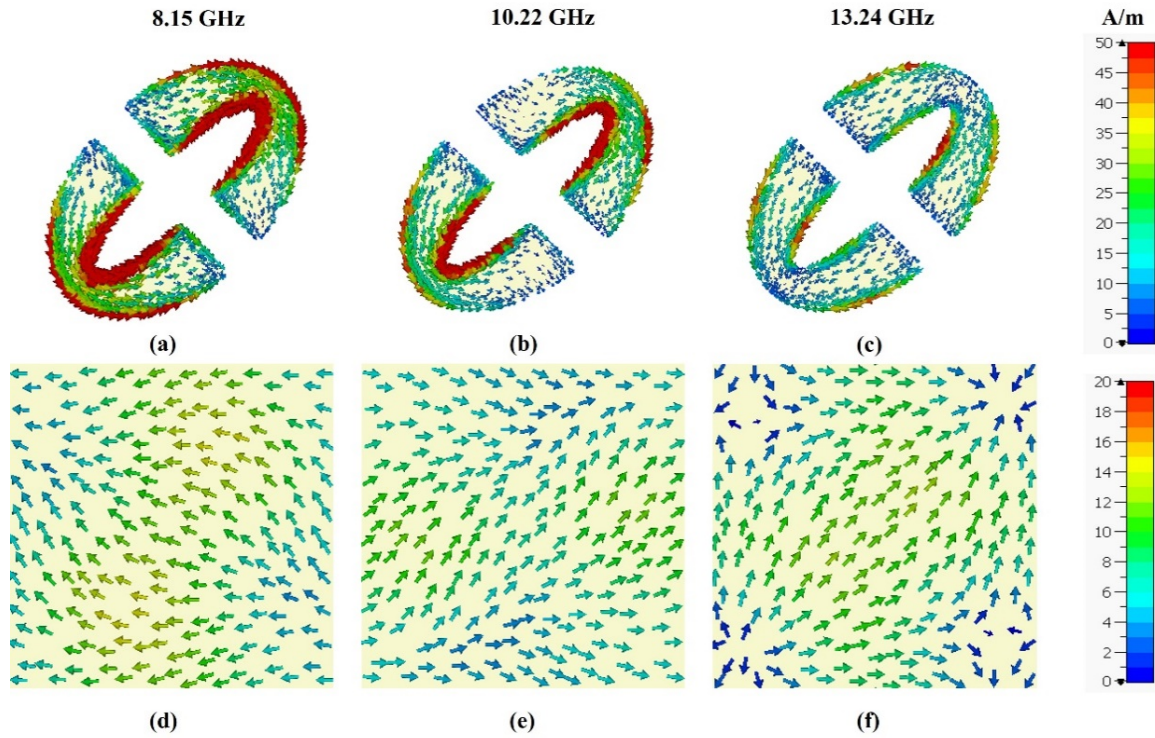


Figure 5. Surface current distributions over top and ground layers of the converter at (a,d) 8.52 GHz, (b,e) 12.78 GHz, and (c,f) 17.44 GHz.

3.2. Surface Current

To further examine the efficiency and performance of the presented meta-surface, we performed a directional analysis of the current density for the top and ground structures at the resonant frequencies. Because of the anisotropy of the unit cell, the applied electromagnetic wave generates current on the connected meta-surface [3]:

$$\begin{bmatrix} J \\ M \end{bmatrix} = i\omega \begin{bmatrix} \alpha_{ee} & \alpha_{em} \\ \alpha_{me} & \alpha_{mm} \end{bmatrix} \begin{bmatrix} E \\ H \end{bmatrix}$$

Here, $M = [M_x, M_y]^T$ and $J = [J_x, J_y]^T$ are the densities of magnetic and electric current, respectively; ω is the angular frequency; and α_{ee} , α_{em} , α_{me} , and α_{mm} are electric and magnetic polarizability.

$$Z(\omega) = \sqrt{\frac{\mu(\omega)}{\epsilon(\omega)}}$$

where, electrical permittivity and magnetic permeability are expressed via $\epsilon(\omega)$ and $\mu(\omega)$ [3]. In addition, $Z(\omega)$ is the surface impedance of the converter. The reflection coefficient, expressed via the symbol R , is given by the following equation [3]:

$$R(\omega) = \frac{Z(\omega) - Z_o}{Z(\omega) + Z_o}$$

where, the free-space impedance, denoted by the symbol Z_0 , is 377Ω and $R(\omega)$ is complex reflection coefficient with both imaginary and real parts. At resonant frequencies, magnetization has a high impedance value and thus produces a high permeability value, $Z(\omega_r) \gg Z_0$. In this case, the reflection coefficient is approximately one, $R(\omega_r) \approx 1$ and therefore proposed meta-surface acts as an artificial magnetic conductor (AMC) or a high impedance surface (HIS) or which is wanted for cross polarization conversion. The anisotropic magnetic property at the meta-surface is provided by anisotropy along the u- and v-axis.

The presented metasurface's current distributions at the resonance frequencies are obtained to understand the resonance behavior of the meta-surface. Fig. 5 presents surface current distributions over both the top layer and bottom layer of the converter at all resonant frequencies of $f = 8.15$ GHz, 10.22 GHz, and 13.24 GHz. It is seen from the surface current distributions in Figs. 5(a)-(f) for these frequencies that the proposed meta-surface has magnetic resonance behavior, because these distributions over the resonator portion and the ground are opposite.

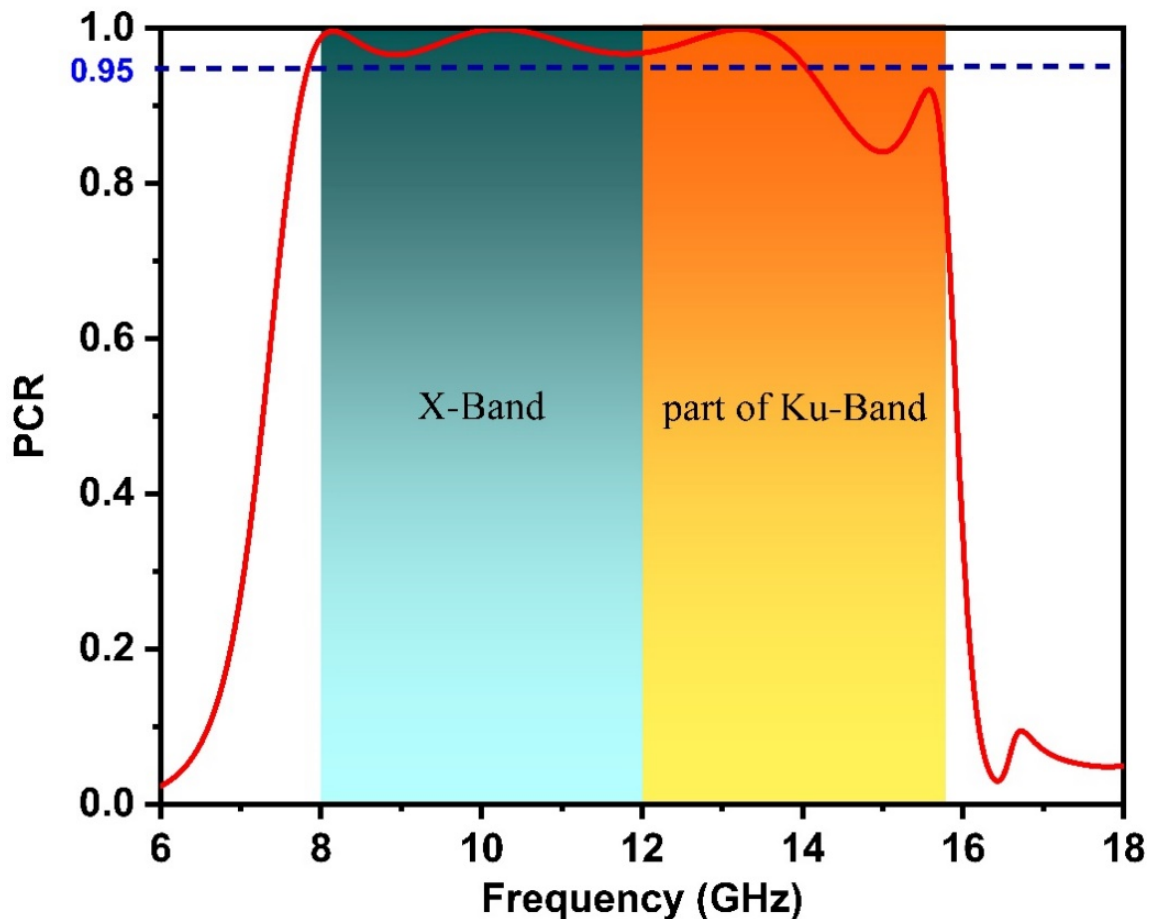


Figure 6. PCR of the suggested meta-surface (normal incidence).

3.3. Polarization Converter Rate (PCR)

The PCR value of the meta-surface is illustrated in Fig. 6. The observed PCR value is greater than 0.97 between 7.89 GHz and 13.91 GHz. This means can be operated as a CPC in the entire X-band. It is also observed that the efficiency of the presented meta-surface can be raised by

operating it around the three different discrete frequencies (8.15 GHz, 10.22 GHz, and 13.24 GHz) because its PCR values approach unity at these frequencies.

Table 2. Comparison with some polarization converters in the literature

Ref No.	Angle Sensitivity	CPC Band (GHz)	Value of PCR Efficiency(%)	RAB (%)	Type of Substrate	Thickness (mm)
[1]	45° (80%)	8-12	> 90	40	FR4	0.04λ ₀
[2]	45° (80%)	12-18	> 90	40	FR4	0.06λ ₀
[4]	45° (80%)	8-11	> 90	31.6	FR4	0.04λ ₀
[20]	N/A	5.7 – 10.3	> 90	57.5	FR4	0.06λ ₀
[21]	N/A	6.67 – 17.1	> 90	87.7	F4B	0.08λ ₀
[22]	N/A	8.34-26.06	> 99.6	103	PREE	0.16λ ₀
[23]	45° (75%) (up to 22.3 GHz)	10.5-29.5	> 90	95	F4BM	0.09λ ₀
This work	45° (80%) (X band)	7.89– 13.91	> 97	55.2	FR4	0.07λ ₀

Additional analysis was performed to analyze the efficiency of the presented converter for the different incidence angle. It is shown in Figs.7(a)-(b) that different incidence angle in values do not affect the PCR values of the presented converter at lower frequencies. For example, the PCR of the converter is greater than 0.82 in X-band range for incidence angle of 45°.

Table 2 exhibits the comparison of our design and other designs in the literature [1, 2, 4, 20, 21, 22, 23] in terms of the functionality (angle sensitivity, the band of cross polarization converter (CPC), value of PCR efficiency, relative bandwidth, type of substrate, type of layer and thickness).

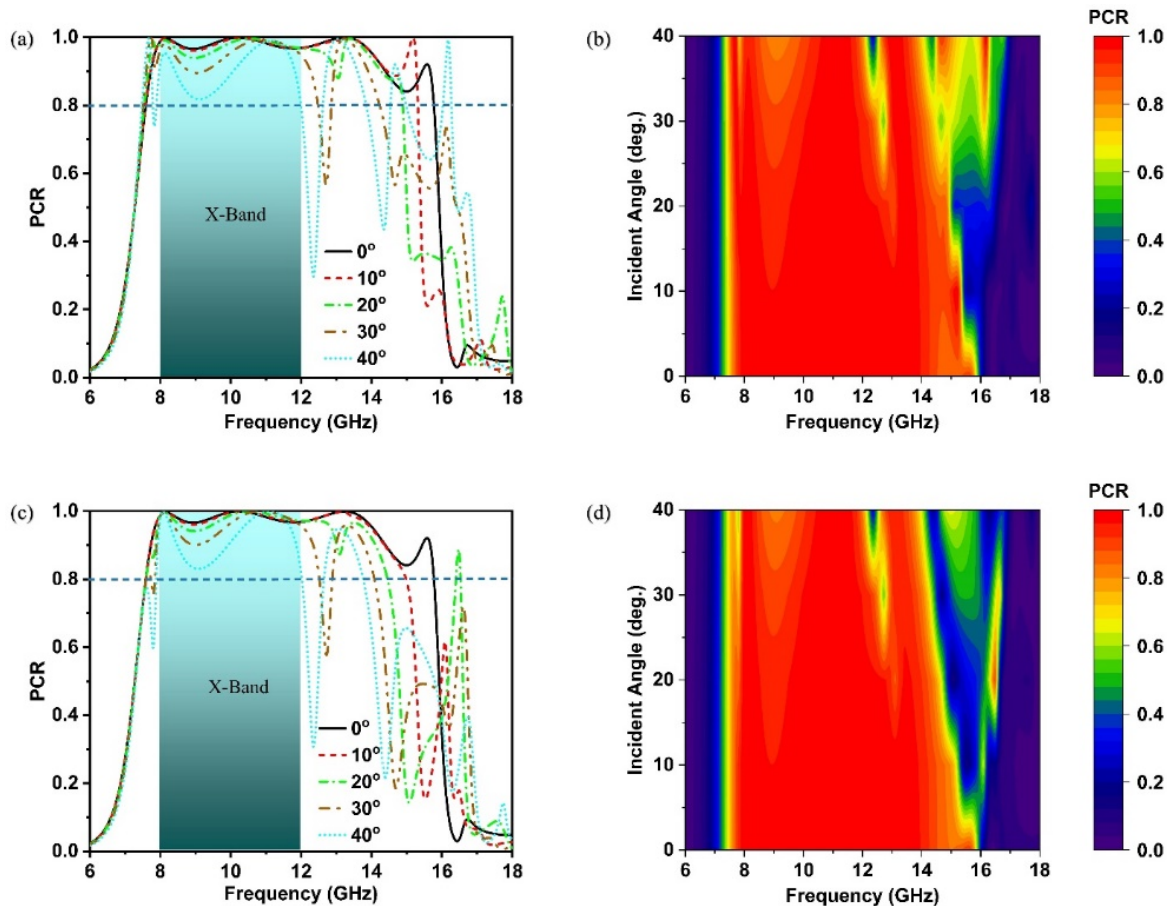


Figure 7. PCR map as a function of frequency and of the incident angle for (a,b) TE and (c,d) TM modes.

4. Conclusion

A single-layer, ultra-thin, wideband, and multi-purpose polarization converter is proposed. It operates as a CPC in the whole of X band and a LP to CP in a part of the C band. It has a PCR efficiency greater than 97% between 7.89 GHz and 13.91 GHz, covering all the X-band with a RAB of 55.2%. Its PCR value is not less than 82% over a wider frequency band (7.9-12 GHz) for incidence angle of 45°. Compared with the polarization converters in the literature, the proposed meta-surface is an important candidate for X-band applications due to its single layer, ultra-thin, simple structure, low cost, easy fabrication, and wide bandwidth features.

Ethics in Publishing

There are no ethical issues regarding the publication of this study.

Author Contributions

Aykut Coskun: converter design, simulations, article writing; Ahmet Teber: evaluation of results; Mehmet Ertugrul: material selection, evaluation of results.

Acknowledgements

This work is financially supported by TUBITAK (The Scientific and Technological Research Council of Turkey) with the Project Number 218M341.

References

- [1] Nguyen, T. K. T., Nguyen, T. M., Nguyen, H. Q., Cao, T. N., Le, D. T., Bui, X. K., Bui, S. T., et al. (2021). Simple design of efficient broadband multifunctional polarization converter for X-band applications. *Scientific reports*, 11(1), 2032.
- [2] Nguyen, T. Q. H., Nguyen, T. K. T., Nguyen, T. Q. M., Cao, T. N., Phan, H. L., Luong, N. M., Le, D. T., et al. (2021). Simple design of a wideband and wide-angle reflective linear polarization converter based on crescent-shaped metamaterial for Ku-band applications. *Optics Communications*, 486(1), 126773.
- [3] Ahmed, F., Khan, M. I., & Tahir, F. A. (2021). A Multi-Functional Polarization Transforming Metasurface for C, X and K band Applications. *IEEE Antennas and Wireless Propagation Letters*, 1(c), 1.
- [4] Khan, M. I., Khalid, Z., & Tahir, F. A. (2019). Linear and circular-polarization conversion in X-band using anisotropic metasurface. *Scientific Reports*, 9(1), 4552.
- [5] Zheng, Y., Zhou, Y., Gao, J., Cao, X., Yang, H., Li, S., Xu, L., et al. (2017). Ultra-wideband polarization conversion metasurface and its application cases for antenna radiation enhancement and scattering suppression. *Scientific Reports*, 7(1), 16137.
- [6] Sun, H., Gu, C., Chen, X., Li, Z., Liu, L., Xu, B., & Zhou, Z. (2017). Broadband and Broad-angle Polarization-independent Metasurface for Radar Cross Section Reduction. *Scientific Reports*, 7(1), 40782.
- [7] Choudhury, S., Guler, U., Shaltout, A., Shalaev, V. M., Kildishev, A. V., & Boltasseva, A. (2017). Pancharatnam–Berry Phase Manipulating Metasurface for Visible Color Hologram Based on Low Loss Silver Thin Film. *Advanced Optical Materials*, 5(10), 1700196.
- [8] Azizi, M. K., Baudrand, H., Latrach, L., & Gharsallah, A. (2017). Metamaterial-Based Flat Lens: Wave Concept Iterative Process Approach. *Progress In Electromagnetics Research C*, 75, 13–21.
- [9] Abdullah, S., Xiao, G., & Amaya, R. E. (2021). A Review on the History and Current Literature of Metamaterials and Its Applications to Antennas & Radio Frequency Identification (RFID) Devices. *IEEE Journal of Radio Frequency Identification*, 5(4), 427–445.
- [10] Qiu, P., Qiu, W., Lin, Z., Chen, H., Ren, J., Wang, J.-X., Kan, Q., et al. (2017). Investigation of beam splitter in a zero-refractive-index photonic crystal at the frequency of Dirac-like point. *Scientific Reports*, 7(1), 9588.

- [11] Park, J., & Min, B. (2021). Spatiotemporal plane wave expansion method for arbitrary space–time periodic photonic media. *Optics Letters*, 46(3), 484.
- [12] Tang, J., Faraz, F., Chen, X., Zhang, Q., Li, Q., Li, Y., & Zhang, S. (2020). A Metasurface Superstrate for Mutual Coupling Reduction of Large Antenna Arrays. *IEEE Access*, 8, 126859–126867.
- [13] Qian, J., Gou, P., Pan, H., Zhu, L., Gui, Y. S., Hu, C.-M., & An, Z. (2020). Hybrid perfect metamaterial absorber for microwave spin rectification applications. *Scientific Reports*, 10(1), 19240.
- [14] Nguyen, T. M., Nguyen, T. K. T., Phan, D. T., Le, D. T., Vu, D. L., Nguyen, T. Q. H., & Kim, J.-M. (2022). Ultra-Wideband and Lightweight Electromagnetic Polarization Converter Based on Multiresonant Metasurface. *IEEE Access*, 10, 92097–92104.
- [15] Gao, X., Han, X., Cao, W.-P., Li, H. O., Ma, H. F., & Cui, T. J. (2015). Ultrawideband and High-Efficiency Linear Polarization Converter Based on Double V-Shaped Metasurface. *IEEE Transactions on Antennas and Propagation*, 63(8), 3522–3530.
- [16] Xu, G., Gao, L., Chen, Y., Ding, Y., Wang, J., Fang, Y., Wu, X., et al. (2022). Broadband Polarization Manipulation Based on W-Shaped Metasurface. *Frontiers in Materials*, 9(3), 1–6.
- [17] Kamal, B., Chen, J., Yingzeng, Y., Ren, J., Ullah, S., & Khan, W. U. R. (2021). High efficiency and ultra-wideband polarization converter based on an L-shaped metasurface. *Optical Materials Express*, 11(5), 1343.
- [18] Mei, Z. L., Ma, X. M., Lu, C., & Zhao, Y. D. (2017). High-efficiency and wide-bandwidth linear polarization converter based on double U-shaped metasurface. *AIP Advances*, 7(12), 125323.
- [19] Salman, M. S., Khan, M. I., Tahir, F. A., & Rmili, H. (2020). Multifunctional Single Layer Metasurface Based on Hexagonal Split Ring Resonator. *IEEE Access*, 8, 28054–28063.
- [20] Zhao, J., & Cheng, Y. (2016). A high-efficiency and broadband reflective 90° linear polarization rotator based on anisotropic metamaterial. *Applied Physics B*, 122(10), 255.
- [21] Xu, J., Li, R., Wang, S., & Han, T. (2018). Ultra-broadband linear polarization converter based on anisotropic metasurface. *Optics Express*, 26(20), 26235.
- [22] Lin, B., Huang, W., Guo, J., Wang, Y., Liu, Z., & Ye, H. (2023). A high efficiency ultra-wideband circular-to-linear polarization conversion metasurface. *Optics Communications*, 529(2), 129102.
- [23] Faraz, Z., Kamal, B., Ullah, S., Aziz, A., & Kanwal, A. (2023). High efficient and ultra-wideband polarization converter based on I-shaped metasurface for RCS reduction. *Optics Communications*, 530(3), 129101.